Pointwise Dimensions of the Lorenz Attractor

Sam Gratrix and John N. Elgin
Department of Mathematics, Imperial College London, 180 Queen's Gate, London SW7 2AZ, United Kingdom
(Received 11 October 2002; published 8 January 2004)

We discuss a connection between two complementary views of the Lorenz attractor: the first is the accepted view where the attractor has a smooth measure on a fractal support. This complex system is alternatively manifest as a self-similar curve for the pointwise dimension alpha. We describe why the latter approach is accessible for the analysis of an experimental signal.

DOI: 10.1103/PhysRevLett.92.014101 PACS numbers: 05.45.Pq, 02.60.Cb

Time series analysis of experimental data often leads to the inference that the effective evolution of the system under observation is primarily controlled by the dynamics of a set of variables spanning a low-dimensional asymptotic attractor [1]. Neither the exact nature of these variables nor their evolution equations are known. However, modern techniques of signal analysis often permit the computation of bounds on the dimension of this attractor, as well as other properties such as the average Lyapunov exponent. Generically, all attractors have a multifractal structure usefully quantified in terms of a spectrum of singularities $f(\alpha)$ [2]. Here $\alpha \in [\alpha_{\min}, \alpha_{\max}]$ is the pointwise dimension of the natural measure μ at point x_i on the attractor and is defined by the relation

$$\alpha(x_i) = \lim_{l_i \to 0} \frac{\ln \mu[S(l_i, x_i)]}{\ln l_i}, \tag{1}$$

where $S(l_i, x_i)$ denotes a segment in an optimum partition and l_i is the diameter of the smallest ball containing S. $f(\alpha)$ is then the Hausdorff dimension of the collection of all points with pointwise dimension α.

One of the earliest and most striking computations of such a spectrum was for an attractor associated with an experimental trajectory on a two-torus with a golden mean winding number obtained from a forced Rayleigh-Bénard system at the onset of chaos [3]. An embedding resulted in a realization of the experimental attractor in $\mathbb{R}^3$ having the appearance of a thin, closed tube. The transverse structure of the tube is necessarily fractal, giving rise to the variation in the values of α. By contrast, one anticipates little variation in α along any one of the fractal "threads" of the tube.

The natural measure for this attractor is a Sinai–Ruelle–Bowen (SRB) measure — that is, there is a smooth variation in the measure along the stretching direction of a thread, and the support for the measure has a singular transverse structure (Cantor set). In view of these statements, it is perhaps remarkable that the authors of Ref. [3] were able to probe the structure of their (experimental) attractor in fine enough detail to enable them to elucidate the multifractal properties. Jensen *et al.* [3] effectively circumvented this difficulty by estimating the measure μ, not from box-counting techniques as suggested by Eq. (1), but rather by relating the measure to an inverse recurrence time for visitations of the trajectory to a ball centered at points x_i on the attractor, then using a partition function to compute $f(\alpha)$. The point here is the association of μ with $1/T_{\text{rec}}$, where T_{rec} is a recurrence time. As the radius of the ball centered at x_i is decreased, the trajectory is necessarily close to a periodic orbit j, say, with period T_j. This is not unlike the association of the pointwise dimension α_j with this periodic orbit, which is very much the approach adopted in this Letter. Here, in a study of the Lorenz system, we argue that the direct computation of the multifractal spectrum of the Lorenz attractor from knowledge of the SRB measure is impractical—because of the difficulties in resolving the structure of the fractal support of the measure in fine enough detail—while a computation from knowledge of the pointwise dimension associated with each periodic orbit supported by the attractor is a practical exercise, as demonstrated elsewhere [4]. Viewed thus, the complexity inherent in the structure of a SRB measure on a fractal support is replaced with a different complexity associated with the self-similar nature of a single curve; this is shown in Fig. 1. The curve displays the variation of the pointwise dimension α computed

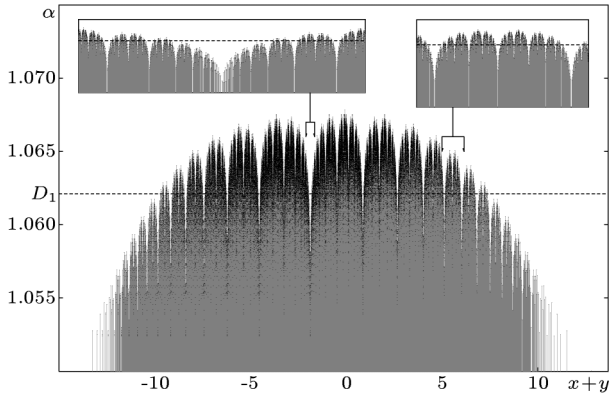

FIG. 1. The pointwise dimension α for periodic points of prime orbits of binary length 2 through 17 of the arc Γ_0 projected onto $x + y$.

 0031-9007/04/92(1)/014101(4)$20.00

from periodic points plotted along a projection of an arc, discussed below, and it is the structure of this curve which is the main concern of this Letter.

Here we are interested in the variation in α along the intersection between the Lorenz attractor [5] and the Poincaré section $z = r - 1$. Specifically, we consider numerical solutions to

$$\dot{x} = \sigma(y - x), \qquad \dot{y} = x(r - z) - y, \qquad \dot{z} = xy - bz, \quad (2)$$

at parameter values $(\sigma, b, r) = (10, 8/3, 28)$. It is well known that this system has a chaotic attractor [6], whose intersection with the plane $z = r - 1$ is shown in Fig. 2. The points F_- and F_+ are the symmetric pair of fixed points $(x, y, z) = (\pm\sqrt{b(r-1)}, \pm\sqrt{b(r-1)}, r - 1)$ of the system (2), while the dashed line Ω passing through the z axis (the origin in Fig. 2) is a representation of the intersection of the two-dimensional stable manifold of the remaining fixed point at the origin with the section. Further intersections of this manifold with the section occur and are discussed below.

The intersecting set, $\Gamma = \Gamma_0 \cup \Gamma_1$, say, has the appearance of two symmetric arcs stretching between F_- and F_+; these are obtained from the intersection points with $\dot{z} < 0$ on the section. The apparent lack of transverse structure on either branch of Γ arises from limited resolution in the figure and is a consequence of the strong dissipation in the Lorenz system. It is well known that the transverse direction is fractal, with a Cantor set structure [7].

The action of the flow on the section is that of a horseshoe, whereby nearby points are expanded in directions along the arc (positive Lyapunov exponent) and contracted in the transverse direction (negative Lyapunov exponent). Accordingly, we have partitioned the section as appropriate for the horseshoe, where the digit before the binary point 0. or 1. indicates which arc the iterate is on, while digits following the binary point indicate further partitioning along the arcs. The flow taking the orbit from one intersection with the section to the next moves the binary point one place to the right [4]. More digits before the point, such as 10. and 00., correspond to a more refined partitioning across the arc Γ_0; for the purpose of this Letter, we need to know only which of the two arcs contains the trajectory, hence the single digit. More digits after the binary point lead to a refinement of the partition along the arc: $0.100 \rightarrow 0.1000 \cup 0.1001$ is a partitioning of 0.100 into smaller segments 0.1000 and 0.1001, both of which are contained within 0.100. In other words, there is a Markov partitioning of the set Γ.

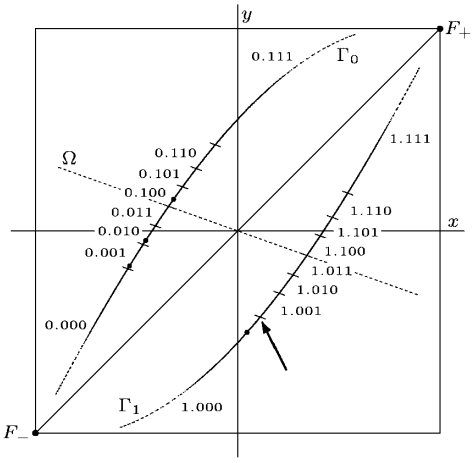

FIG. 2. The Poincaré section is the square with opposite corners at F_- and F_+. The partitioning to level four is shown, and the binary length four periodic orbit $\overline{0.001}$ is indicated by the dots. The dashed line Ω represents schematically the first intersection of the stable manifold of the fixed point at the origin with the section. The arrow points to the intersection $1.000 \cap 1.001$; see text for details.

Now consider what we will loosely call an *edge* between segments. For example, the edge between 0.1000 and 0.1001 is the set $0.1000 \cap 0.1001$, which owing to the transverse structure on Γ_0 is in reality a fractal dust. All such edges result from further intersections of the two-dimensional stable manifolds of the fixed point at the origin with Γ_0 on the surface of section $z = r - 1$. Such an intersection occurs at the edge $1.000 \cap 1.001$, as shown in Fig. 2. It is a direct consequence of this infinite number of intersections that gives α the complicated fractal variation along the arc shown in Fig. 1. The left inset shows the self-similar structure centered around $0.0 \cap 0.1$—that is, in the vicinity of the intersection of Γ_0 with Ω. Note that the structure of the right inset replicates that of the full figure. We now discuss how this curve was obtained.

A "typical" estimate of the dimension of the Lorenz attractor using standard box-counting techniques Eq. (1) will result in a value for $\alpha = D_1$ (the information dimension) $= 1.062\cdots$. That is, with respect to the natural measure on the attractor, $\alpha(x)$ takes the common value quoted for almost every point x. Generically, a chaotic attractor has a countable dense set of unstable periodic orbits embedded within it. Grebogi *et al.* [8] demonstrate that, for points chosen close to the stable or unstable manifolds of such orbits, $\alpha(x)$ differs from D_1. Focusing on such periodic orbits, they then introduce the notion of pointwise dimension α_j for points on the jth-periodic orbit in terms of the characteristic (Floquet) multipliers for this orbit. For the Lorenz system, this reads

$$\alpha_j = 1 - \frac{\ln\Lambda_j}{\ln\lambda_j}, \quad (3)$$

where $\Lambda_j > 1 > \lambda_j$ are the multiplier magnitudes. Wiklund and Elgin demonstrate how explicit results for α for each periodic orbit can be appropriately averaged to produce the required singularity spectrum [4].

The basic idea is as follows: continued refinement of the partition along Γ_0 will produce segments with binary string of arbitrary length. A string sequence indefinitely repeated corresponds to a periodic orbit. The procedure

then is to find all periodic points below some maximal binary length along Γ_0, compute α_j for such points in accordance with Eq. (3), then display the results in relation to the periodic points graphically, as in Fig. 1. In carrying out this procedure, only *prime* periodic orbits need be considered. These are periodic orbits of length n, say, which are not repeats of orbits of shorter binary length. All such orbits to binary length 17 are included in Fig. 1, where we parametrize points along Γ_0 by $x + y$. Details on how such periodic points were obtained are discussed below. For the moment, we emphasise the self-similar nature of the variation of α along the arc and remind the reader that the origin for this is the countable infinity of intersections of the two-dimensional stable manifold of the origin with the section $z = r - 1$.

The action of the horseshoe on the section is often likened to that of the Baker's map (SRB measure), replicating the stretching and folding action found in the Lorenz system. Essentially, this is a refinement of a simple Cantor set into two segments, l_a and l_b, say, with phenomenologically associated probability measures p_a and p_b. The partition function

$$1 = \lim_{n\to\infty} \sum_{i=1}^{(n)} \frac{p_i^q}{l_i^\tau},$$

where n is the level of refinement of the Cantor set and q and $\tau(q)$ are the usual thermodynamic variables, can be evaluated explicitly. Solving the transcendental equation

$$\frac{p_a^q}{l_a^\tau} + \frac{p_b^q}{l_b^\tau} = 1 \tag{4}$$

for $\tau(q)$ allows one to compute $f(\alpha)$ in the usual way. The association of p_i^q/l_i^τ with $\lambda^{q-\tau-1}/\Lambda^q$ [8] permits direct computation of the curve $f(\alpha)$ from periodic orbits supported by the map [4].

To complete this picture, we now consider how α varies with an ordering of the periodic points. To do this, we return to the Lorenz system. Figure 1 indicates that the variation in α, as computed using periodic orbits, within any ball centered at a point on the arc Γ_0 always has a self-similar structure irrespective of the radius of the ball. We may, consistent with Eq. (1), now compute an average over all such periodic points within the ball taken in the limit where the diameter of the ball is taken to zero; call this $\langle\alpha_j\rangle(x)$, which varies smoothly along Γ_0. Recently, the measure introduced in connection with a return map $f(x)$ for a geometric model of the Lorenz attractor was shown to be a SRB measure [6].

Shown in Fig. 3 is a different estimate for $\alpha(x)$ obtained in a manner more in keeping with that used by Jensen *et al.* [3]. These authors estimate μ [as appears in our Eq. (1)] as the inverse recurrence time for visitations of the orbit to a ball centered at x_i, then use a partition function to compute α and $f(\alpha)$. As mentioned previously, the point here is the association of μ with $1/T_{\rm rec}$, where $T_{\rm rec}$ is a recurrence time. Here we modify their procedure slightly and attribute to points on Γ_0 a measure determined by a recurrence time to the section. Specifically, for a set of arbitrary points on Γ_0 we compute

$$\beta = \lim_{n\to\infty} \frac{T_{\rm rec}}{n},$$

where $T_{\rm rec}$ is now the time taken for the nth return to the section. The limit is equivalent to computing a value for β from a return time to a ball of radius l centered at point x taken in the limit $l \to 0$, as computed by Jensen *et al.* [3]. For the subset of periodic points on the arc the limit is simply equal to the period of the orbit divided by the binary length. Since we have at hand a large and accurate collection of periodic orbit data, we have constructed the β curves of Fig. 3 using this information only. The curves of Figs. 1 and 3 show a close correspondence in their self-similar structure, indicating that the use of recurrence time to compute a multifractal spectrum is an excellent approximation to computing the same spectrum from periodic orbits, more so when the latter are not known — as for the case of an experimental signal.

Interpreting Fig. 3 as a set of experimental data, D_1 may be directly computed by covering the arc Γ_0 with balls of diameter l, where the average value of β within ball i defines the quantity β_i. A value for D_1 is then obtained by computing $\sum_i \beta_i^{-1} \ln\beta_i^{-1}/\ln l$, in the limit $l \to 0$. The construction of the $f(\alpha)$ spectrum from the experimental data, following Ref. [3], will provide greater information about the attractor, including a value for D_1. However, noise contained within real data will limit the resolution of the fine structure in Fig. 3, although this seems not to impede the computation of $f(\alpha)$ as demonstrated in Ref. [3].

Figure 4 presents the α plots for increasing maximal binary length. We see that as binary length is increased — at least until $N_p = 17$ — the effect is to fill out the plot in the wings. Investigation at greater lengths is currently being undertaken, which is problematic due to the combinatorial explosion in the number of periodic points. We

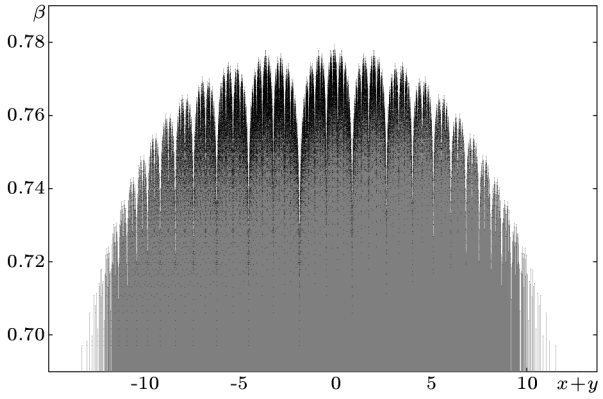

FIG. 3. The recurrence measure β for periodic points of prime orbits of binary length 2 through 17 of the arc Γ_0 projected onto $x + y$.

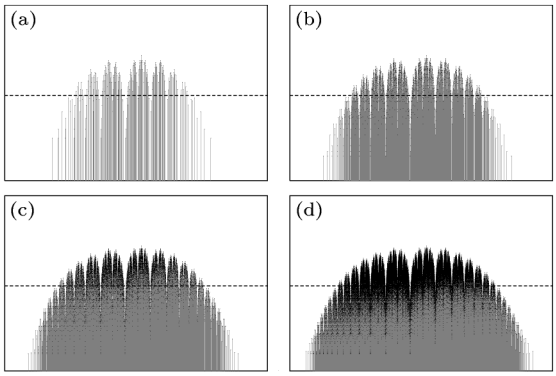

FIG. 4. The pointwise dimension along Γ_0 with increasing maximum binary orbit length N_p: (a) $N_p = 8$, with 235 periodic points; (b) $N_p = 11$, 2005 periodic points; (c) $N_p = 14$, 16 237 periodic points; (d) $N_p = 17$, 130 777 periodic points.

now describe in more detail the technique for computing the periodic orbits.

The method employed to find all prime orbits to string length $N_p = 18$ is similar to that in Ref. [4]. We choose a point and integrate forward in time, which will yield a (chaotic) trajectory on the attractor. The encoding of this general trajectory is generated by recording the digit 0 when the fixed point F_- is encircled, digit 1 for F_+, consistent with our encoding of the horseshoe. If this binary stream contains a substring comprised of some repeats of the prime string $s_1 s_2 \cdots s_n$, we know by shadowing arguments that the corresponding portion of the trajectory is near a periodic orbit p of binary length n. One section with the same binary code as p is then used as an initial mesh for a boundary value problem (BVP) routine, which, if convergent, will return the periodic orbit with symbolic encoding $\overline{s_1 . s_2 \cdots s_n}$. Each periodic point of p is then determined by choosing the nearest calculated point before the section is reached, integrating forward, and taking a final Hénon step to land precisely on $z = r - 1$.

To obtain the multipliers, the monodromy matrix $\mathbf{J}_T$ must be calculated. The Lorenz system is extended to include the nine equations of the evolution of the Jacobian of the flow $\dot{\mathbf{J}} = \mathbf{V}\mathbf{J}$, where $\mathbf{V}$ is the derivative matrix of the right-hand side of Eq. (2). Choosing a periodic point of p as an initial condition, we now integrate this new system to find $\mathbf{J}_t$ for $t \in [0, T]$ using a standard initial value problem routine. This provides an approximate mesh for the extended Lorenz system from which we may accurately find $\mathbf{J}_T$ using a BVP code.

When Λ_j/λ_j for long orbits becomes too large, the routine fails. Then, in general, we may break our problem into m smaller boundary value problems, where $m \in [20n, 40n]$. We take m samples at times t_i from the solution mesh of p and solve the extended system on the intervals $[t_i, t_{i+1}]$, $i = 0, \ldots, m-1$, each with the initial condition $\mathbf{J}_0 = \mathbf{I}$ and boundary conditions taken from p. Note that in this case rather than using a BVP routine taking an initial mesh, a BVP routine requiring only the interval end points is needed, since the solution on each interval is much more tractable. The resulting m matrices are then multiplied out evenly to give $\mathbf{J}_T$.

The above calculations were performed on an AMD Athlon processor using 16 decimal digit precision. The BVP codes used were the finite-difference based routines D02RAF and D02GAF provided by the Numerical Algorithms Group; the tolerance used for finding the orbits was 10^{-10}. For all orbits, the monodromy matrix was calculated using both methods described above, with the error in the unit multiplier (the multiplier along the orbit) used to determine the more accurate solution. The first method with tolerances 10^{-8} to 10^{-10} generally fails for binary lengths greater than 13, but otherwise was found to be more accurate than the second. With the second method, it was possible to determine the multipliers of long near-homoclinic orbits such as $\overline{1.1^{16}0^{20}}$, which gave an error of less than 10^{-5} in the unit multiplier, even though $\Lambda_j/\lambda_j \approx 10^{170}$.

In conclusion, we have discussed the connection between two complementary views of the Lorenz attractor: the first is the standard view, where the attractor has a fractal support and a SRB measure. This complex system is alternatively manifest as a self-similar curve where the pointwise dimension α for periodic points is plotted along the arc Γ_0. These models complement each other in the sense that either can be used to compute the multifractal spectrum for the attractor. Further, we have discussed the similarity between an approximation based on periodic orbits and one where a partition function is constructed from knowledge of recurrence times T_{rec} to a ball on a surface of section. It is this last approach which is most accessible to the experimentalists—as demonstrated in the work of Jensen *et al.*—through which it is possible to explore the multifractal nature of the underlying attractor in the experimental system.

More plots may be found at http://gratrix.net/lorenz.

S. G. thanks EPSRC for financial support.

[1] D. S. Broomhead and G. P. King, Physica (Amsterdam) **20D**, 217 (1986).
[2] T. C. Halsey, M. H. Jensen, L. P. Kadanoff, I. Procaccia, and B. I. Shraiman, Phys. Rev. A **33**, 1141 (1986).
[3] M. H. Jensen, L. P. Kadanoff, A. Libchaber, I. Procaccia, and J. Stavans, Phys. Rev. Lett. **55**, 2798 (1985).
[4] K. O. Wiklund and J. N. Elgin, Phys. Rev. E **54**, 1111 (1996).
[5] E. N. Lorenz, J. Atmos. Sci. **20**, 130 (1963).
[6] W. Tucker, Found. Comput. Math. **2**, 53 (2002).
[7] C. Sparrow, *The Lorenz Equations: Bifurcations, Chaos, and Strange Attractors* (Springer-Verlag, New York, 1982).
[8] C. Grebogi, E. Ott, and J. A. Yorke, Phys. Rev. A **37**, 1711 (1988).